

## 27. FERROMAGNETIC FRACTION OF CRETACEOUS AND CENOZOIC SEDIMENTS OF THE RIO GRANDE RISE AND BRAZIL BASIN<sup>1</sup>

G. N. Petrova and T. B. Nechaeva, Institute of Physics of the Earth Academy of Sciences of the U.S.S.R., B. Gruzinskaya 10, Moscow 123810, U.S.S.R.

G. Z. Gurary, Geological Institute, Academy of Sciences of the U.S.S.R., Pyjevsky 7, Moscow 109017, U.S.S.R. and

V. A. Chmerv, Institute of Physics of the Earth Academy of Sciences of the U.S.S.R., B. Gruzinskaya 10, Moscow 123810, U.S.S.R.

### ABSTRACT

Investigation of the ferromagnetic fraction of sediments from the Brazil Basin and Rio Grande Rise shows that its main constituents are magnetite and hematite. The magnetite is detrital, but the hematite is both detrital and chemical in origin. Magnetite is the main carrier of the natural remanent magnetization (NRM); therefore, the NRM is detrital remanent magnetization (DRM). In a number of cases, the change of magnetic parameters along the stratigraphic column permits some refinement of the previously defined boundaries of the lithologic units.

### INTRODUCTION

At present, paleomagnetic investigations are particularly important in stratigraphic studies, both for intraregional and interregional correlations. Depending on its origin, natural remanent magnetization (NRM) can be synchronous with the process of rock formation; detrital remanent magnetization (DRM) and primary chemical remanent magnetization (CRM) changes can arise at any time after the formation process is over (for example: secondary CRM or viscous remanent magnetization). Secondary magnetization can modify and sometimes fully change primary paleomagnetic characteristics; these changes may lead investigators to erroneous conclusions.

The present report describes the composition and origin of ferromagnetic minerals, those carrying NRM, from the Eocene to Quaternary sediments from Hole 515B (Brazil Basin) and Cretaceous to Miocene sediments from Hole 516F (Rio Grande Rise), both drilled during Deep Sea Drilling Project Leg 72. We focus primarily on the change in composition and quantity of the ferromagnetic minerals in our samples.

### METHODS

This investigation is based on a completely new suite of samples, not treated in laboratories before. The following magnetic methods were used:

1) Differential thermomagnetic analysis (DTMA): the rate of change of saturation magnetization ( $J_s$ ) with respect to temperature— $\Delta J_s/\Delta t^\circ(t^\circ)$ —at the first and the second heatings up to 700°C (Burov and Yasonov, 1979);

2) Usual thermomagnetic analysis: the dependence of the change in saturation magnetization ( $J_s$ ) on temperature— $J_s(t^\circ)$ —at the first and second heatings up to 700°C;

3) The method of saturation parameters: the change of saturation remanent magnetization ( $J_{rs}$ ) and remanent coercive force ( $H_{cr}$ ) after

heating, cooling, and a new magnetization; at each new heating, the temperature was increased by 100°C (Petrova, 1977);

4) The determination of dependence of remanent magnetization ( $J_r$ ) on magnetic field  $H$  and  $H_{cr}$ ;

5) The determination of coercive spectra (CS) of Ir.

Investigations relating to the last two points were mainly carried out with samples that were first heated to  $t = 280^\circ\text{C}$  during thermal cleaning for paleomagnetic studies. A lack of available samples necessitated this reuse; however, our results bear out the validity of using such samples.

DTMA, dependence of  $J_r(h)$ , and  $H_{cr}$  were carried out on 37 samples from Hole 515B and 51 samples from Hole 516F;  $J_s(t^\circ)$  curves, saturation parameters, and CS were defined for a few samples (eight samples from Hole 515B and 15 from Hole 516F) in order to fully characterize groups of samples with typical DTMA curves.

### RESULTS

All initial curves  $\Delta J_s/\Delta t^\circ(t^\circ)$  and  $J_s(t^\circ)$  have characteristics typical for paramagnetic minerals. The presence of ferromagnetic minerals in the above samples is absolutely clear, because the samples possess NRM intensities of  $10^{-6} \pm 10^{-7}$  emu, as well as saturation isothermal remanent magnetization (sIRM) of  $10^{-4}$  emu, in spite of the dominance of paramagnetic minerals in the curves. Saturation IRM of paramagnetic minerals is more intense than that of ferromagnetic ones, and Curie points of the ferromagnetic minerals are barely detected because of change of paramagnetic  $T_s(t^\circ)$  in the temperature interval, where  $T_c$  can be expected. According to DTMA curves, the studied samples can be divided into four groups:

1) Samples that show intense formation of new ferromagnetic minerals during heating (Fig. 1A) (these samples mainly occur in the upper parts of the sedimentary column, although hints of this process are noticed in samples from greater sub-bottom depths as well);

2) Samples in which new ferromagnetite mineral does not form during fast heating (about 50°/minute) (Fig. 2A);

3) Samples that contain maghemite;

<sup>1</sup> Barker, P. F., Carlson, R. L., Johnson, D. A., et al., *Init. Repts. DSDP*, 72: Washington (U.S. Govt. Printing Office).

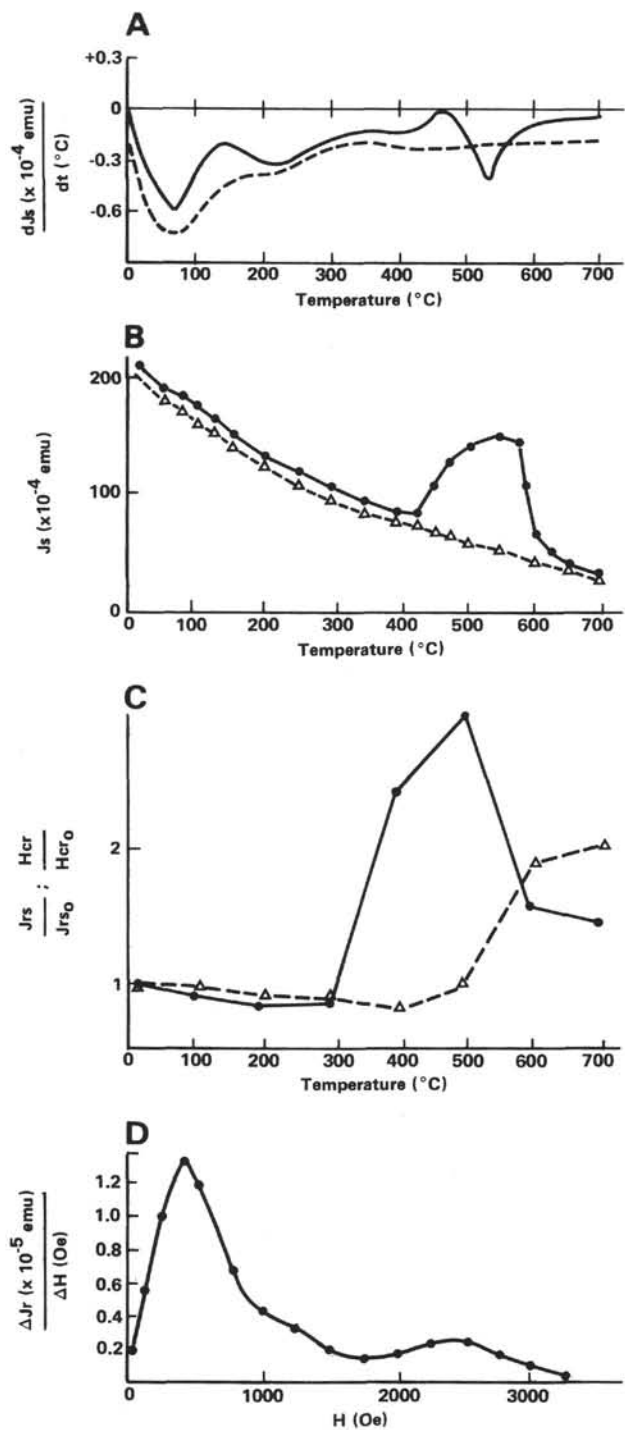


Figure 1. Composition of ferromagnetic minerals for typical sample of Group 1 (515B-46-1, 41-43 cm). A. Differential thermomagnetic analysis; solid line indicates data taken after the first heating; dashed line indicates data taken after the second heating. B. Change of saturation remanent magnetization (Jrs); solid dots: first heating; triangles: second heating. C. Change of saturation parameters Jrs and Hcr (remanent coercive force) after progressive heatings. (Measurements of Jrs and Hcr are made after heating to definite temperature and cooling to room temperature.) Solid circles = Jrs; triangles = Hcr. D. Coercive spectrum (unheated sample). dJs = rate of change of saturation magnetization; t = temperature; subscript o = original; Jr = remanent magnetization; H = field strength.

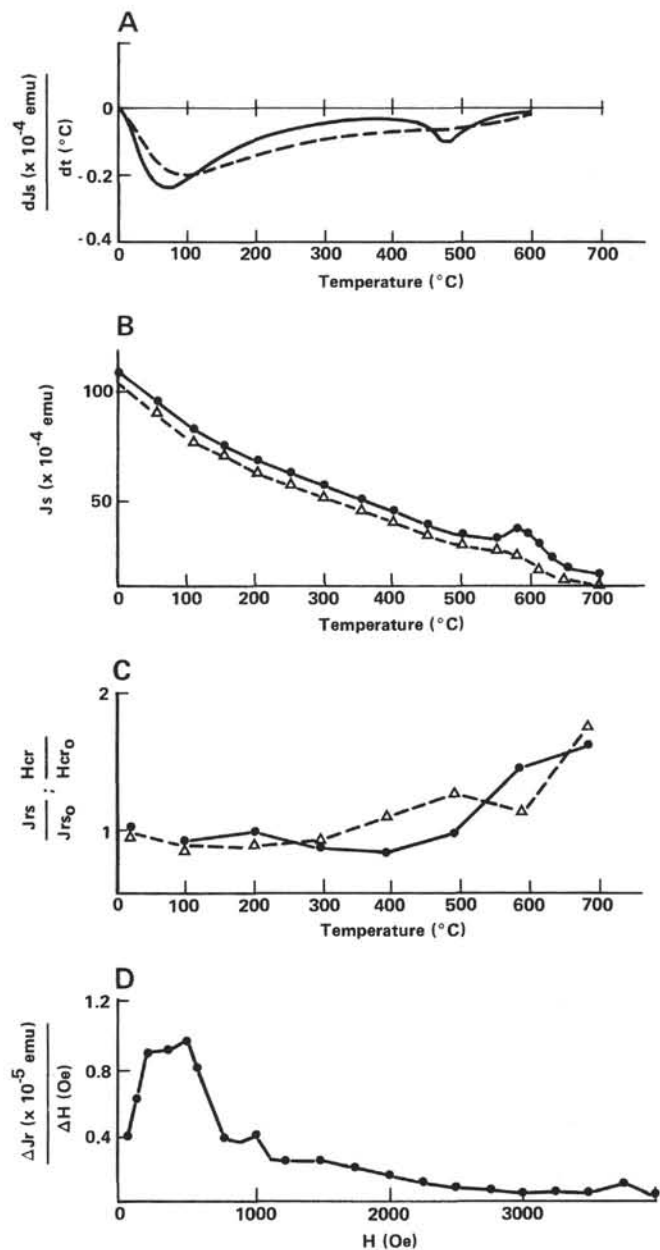


Figure 2. Composition of ferromagnetic minerals for a typical sample of Group 2 (515B-38-4, 87-89 cm). (A-D and abbreviations as in Fig. 1.)

4) Samples that have typical paramagnetic curves (Fig. 3A).

The distributions of the different kinds of samples in the holes are represented in Figure 4C.

In our study, the diagnosis of ferromagnetic minerals is complicated. A typical DTMA curve for the first groups of samples is given in Figure 1A. Minima between 80 and 240°C are caused by dehydration (Burov and Yasonov, 1979). Most curves show this effect, even though intensity changes from one sample to another and the effect has the tendency to decrease with the increasing sub-bottom depth. After 300°C,  $\Delta J_s/\Delta T^\circ$  begins to increase, reflecting the intensive formation of

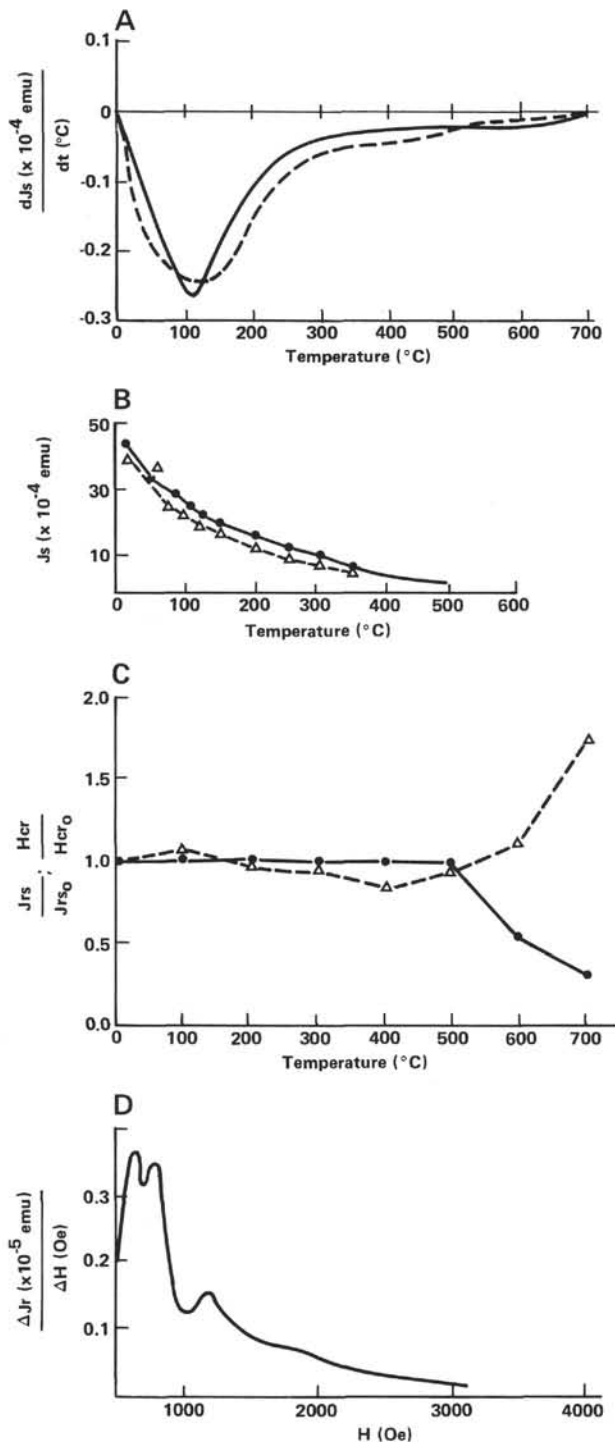


Figure 3. Composition of ferromagnetic minerals for a typical sample of Group 3 (516F-82-2, 92-94 cm). (A-D and abbreviations as in Fig. 1.)

a new ferromagnetic mineral (Fig. 1A). The maximum of this process is reached at a temperature of  $500 \pm 20^\circ\text{C}$ ; then the curve declines sharply, indicating destruction of the ferromagnetic grains, approach of the Curie point ( $T_c$ ), or both. A minimum is reached at  $560 \pm 20^\circ\text{C}$ ; then the curve approaches the zero line. For the samples of the second group,  $J_s(t^\circ)$  of ferromagne-

tite is not decreased by the formation and destruction of new ferromagnetic minerals (Fig. 2). The DTMA method estimation of  $T_c$ , taking the maximum of the second derivative,<sup>2</sup> is near to the  $T_c$  of magnetite. The same occurs with the samples of the third group (Fig. 3).

For convenience of interpretation of the  $\Delta J_s/\Delta t^\circ$  results, histograms of distribution of temperature intervals were drawn, in which  $T_c$  of the ferromagnetic minerals in samples from the first three groups are present (Fig. 4). The extreme right column of each histogram indicates the number of cases in which  $T_c$  could not be determined because of a considerable predominance of paramagnetic components (samples of Group 4). Sharp maxima of the histograms for both holes correspond to the temperatures of the  $T_c$  (about  $580^\circ\text{C}$ ) of magnetite (Figs. 4A-B). Magnetite is present in samples of all the three groups (Figs. 1-3). Although hematite occurs in a number of samples, magnetite is likely to be the main ferromagnetic mineral; two-thirds of the samples from Hole 515B and three-fourths of the samples from Hole 516F register no hematite (Fig. 5).

The paramagnetic character of the  $J_s(t^\circ)$  and  $\Delta J_s/\Delta t^\circ$  curves for samples from the lower part of Hole 516F (Group 4, samples from the Cretaceous) prevents discovery of the initial ferromagnetic  $T_c$ , and suppositions regarding the composition of the ferromagnetic fraction are made only on the basis of changes of saturation magnetization. At temperatures above  $500^\circ\text{C}$  in these samples,  $H_{cr}$  falls from more than 2000 Oe to between 300 and 500 Oe;  $J_{rs}$  increases by a factor of 2 to 3; and  $J_s$  increases by 10 to 40% (Fig. 3C). Such trends of saturation parameters at initial  $H_{cr}$  greater than 2 kOe are possible for hydroxides, although destruction of hydroxides usually occurs at lower temperatures. Because this part of Hole 516F lacks an age analogy in Hole 515B, it will not be discussed further.

Thus, magnetite and hematite are the main ferromagnetic minerals throughout most of Holes 515B and 516F; samples of lower parts of Hole 515B also have maghemite, and Cretaceous samples from Hole 516F have hydroxides.

Before considering possible origins of these ferromagnetic minerals, we should determine if some of these are formed by laboratory heating. Because the product is very unstable, it is unlikely that it is either magnetite or hematite. Repeated heating produced a trend for  $J_s(t^\circ)$  that indicates no traces of new minerals (Figs. 1A and 1C). The curves of saturation parameters (Fig. 1C) show that its formation begins after  $300^\circ\text{C}$  and that it is destroyed completely by  $500^\circ\text{C}$ . The appearance of this ferromagnetic mineral at a temperature of  $400^\circ\text{C}$  makes  $J_{rs}$  increase 2-20 times. After it is destroyed,  $J_{rs}$  returns to almost its initial value. At first  $H_{cr}$  decreases by

<sup>2</sup> In the DTMA method,  $T_c$  is estimated by the maximum of the second derivative of  $J_s(t^\circ)$ . In figures of this paper, the first derivative of  $J_s(t^\circ)$  is given, i.e.,  $T_c$  can be estimated by the most pronounced rate of increase of  $dJ_s/dt$ . For the first group of samples (Fig. 1A), it is difficult to be sure of the correct estimate of  $T_c$  because of the formation of new ferromagnetic minerals in temperature interval of  $400-500^\circ\text{C}$ . The increase of  $dJ_s/dt$  in the interval of  $550-600^\circ\text{C}$  is a result of this process. The samples of the third group (Fig. 3A) have the curves typical for paramagnetic minerals, but samples of the second group are somewhat disturbed by a new ferromagnetic mineral, producing a  $T_c$  in the interval between 550 and  $650^\circ\text{C}$ . The same picture can be seen in the curves for  $J_s(t^\circ)$  (Figs. 1B, 2B, 3B).

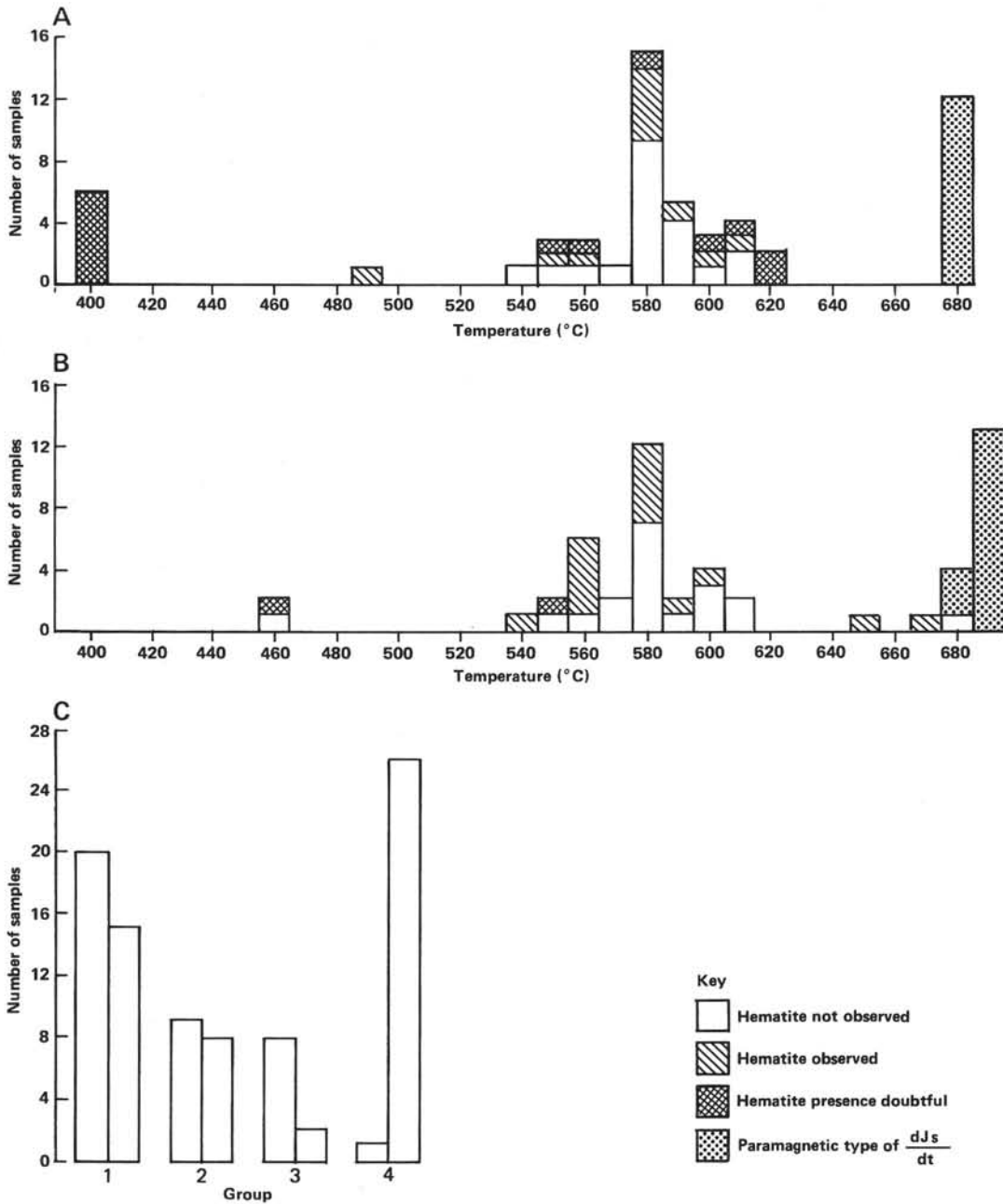


Figure 4. Distribution of Curie point ( $T_c$ ) estimated by differential thermomagnetic analysis. A: Hole 515B, B: Hole 516F, C: distribution in Hole 515B (the left bar of each pair) and 516F (the right bar of each pair) of samples of different types: (1) samples in which laboratory heating formed a new ferromagnetic mineral (see Fig. 1), (2) samples in which ferromagnetic minerals did not form (see Fig. 2), (3) samples in which maghemite was present, and (4) samples in which the paramagnetic parts of thermocurves did not allow determination of  $T_c$  (see Fig. 3).

30–50%, characteristic of the early stage of formation of new ferromagnetic grains (particularly their supermagnetic part). Then  $H_{cr}$  increases; the rate for soft samples is twice as great as that for hard samples. A distinct trace of hematite appears in some DTMA curves (Fig. 5F). Similar changes of magnetic properties in the same temperature interval were observed when siderite, lepidocrocite, and other minerals are destroyed (Rybak, 1971; Bagin et al., 1974). Laboratory heating, therefore,

does not lead to the appearance of magnetite as a new ferromagnetic mineral but can lead to the formation of hematite. Perhaps hematite, or some portion of it, was formed in the sediments as a result of *in situ* heating.

We can assume the following origin of the most important potential carriers of NRM:

1) Magnetite is the primary ferromagnetic mineral in these sediments. Its origin can be either detrital, introduced by the breakdown of magnetite-bearing parent

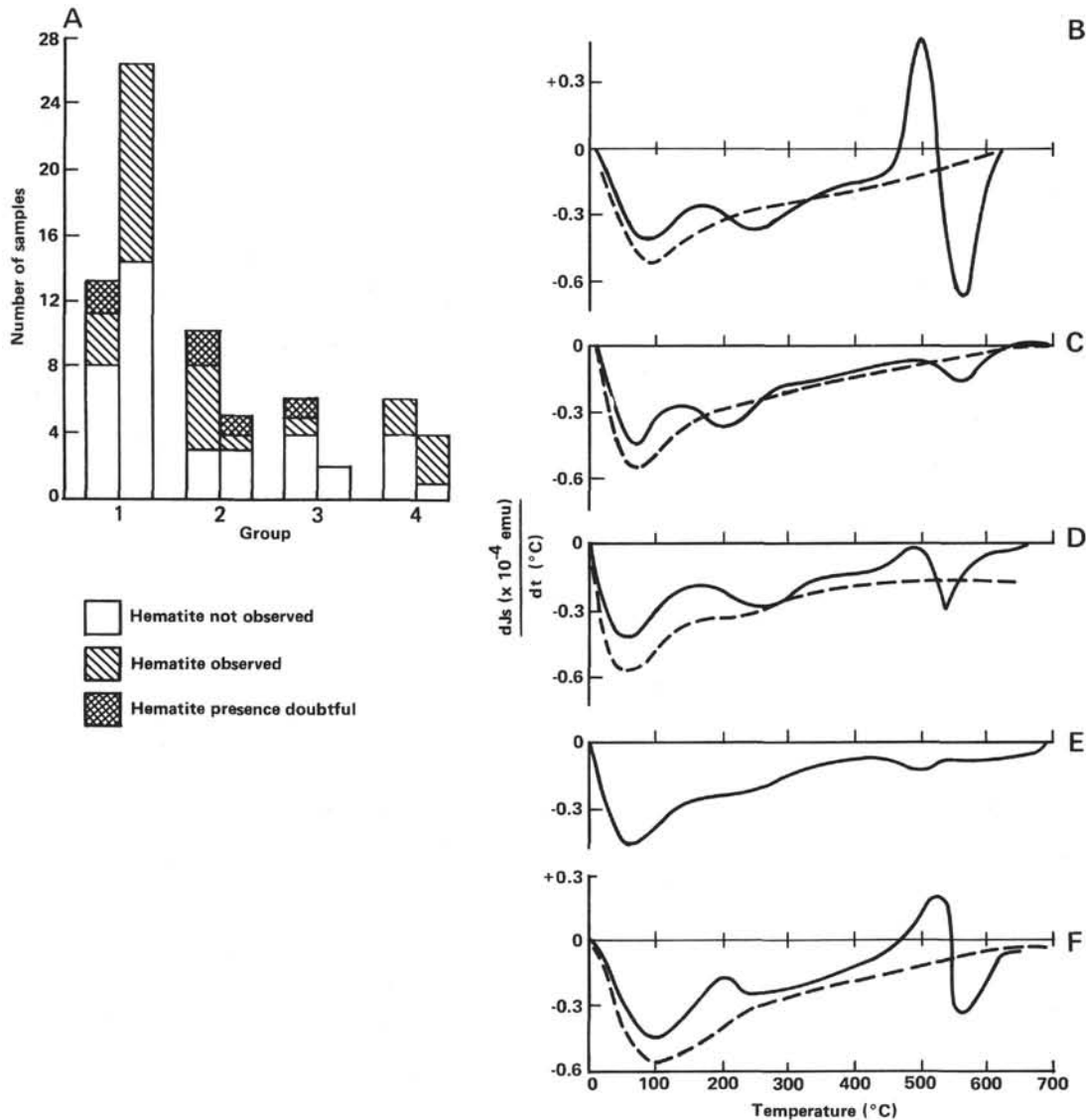


Figure 5. A. The presence of hematite in samples from Hole 515B (the left bar of each pair) and Hole 516F (the right bar of each pair). B. Group 1, no hematite (Sample 515B-50-1, 55-57 cm). C. Group 2, apparently no hematite, but irregularities of the curve do not allow us to be sure (Sample 515B-46-5, 89-91 cm). D. Group 3, the curve  $dJ_s/dt^\circ$  approaches asymptotically to the abscissa in the temperature region of 620-660°C (Sample 516F-29-1, 56-58 cm). E. Group 4, hematite is present (Sample 516F-51-4, 104-106 cm). F. Hematite appears after destruction of new ferromagnetic (Sample 516F-23-2, 65-67 cm).

Thermomagnetic Curves B-E correspond to Columns 1-4 of the histograms. Dashed curves represent second heating; solid curves represent first heating.

rocks of neighboring terrains, by volcanic fallout, or by chemical processes introduced at early stages of the formation of the rocks.

2) Hematite results from the natural process of paramagnetic mineral transformation, a process that also occurs during the course of laboratory heating. It can also be a product of magnetite oxidation and even have a partially detrital origin.

3) The maghemite in the lower part of Hole 515B is associated with oxidation of primary magnetite, supporting the interpretation that the hematite is secondary.

4) The hydroxides present in great amounts in the lower part of 516F are most likely of secondary origin.

Hcr for all samples are compiled in the histograms of Figure 6, Hcr values range mainly from 300 to 900 Oe; values of 500 to 600 Oe predominate. These values indicate that the magnetite present has mainly small but multidomain grains.

Hcr from 1200 to 3800 Oe are observed only in the lower part of Hole 516F, in the Cretaceous sediments (Table 1). As mentioned above, the change of the saturation parameters with heating shows that the rocks contain hydroxides. After the hydroxides are destroyed at temperatures of 500-700°C, Hcr falls to 200-400 Oe. Structural peculiarities of ferromagnetic grains are well reflected by coercive spectra (CS) curves (Figs. 1D, 2D,

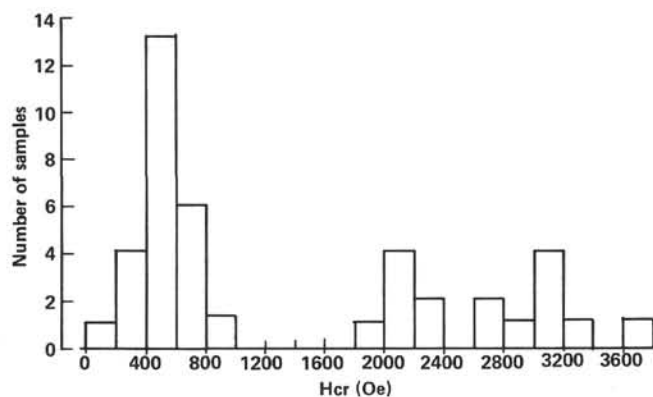


Figure 6. Distribution of remanent coercive force (Hcr) in the samples from Hole 516F.

Table 1. Magnetization data for Hole 516F.

| Core-section<br>(interval in cm) | Hc<br>(Oe) | Jr<br>( $\times 10^{-6}$ emu) | Jrs<br>( $\times 10^{-6}$ emu) |
|----------------------------------|------------|-------------------------------|--------------------------------|
| 19-2, 103-105                    | 600        | 0.1                           | 100                            |
| 22-1, 48-50                      | 700        | 0.1                           | 220                            |
| 25-2, 34-36                      | 500        | 0.1                           | 180                            |
| 26-1, 86-88                      | 350        | 0.4                           | 700                            |
| 27-3, 8-10                       | 400        | 0.1                           | 250                            |
| 29-1, 56-58                      | 400        | 0.1                           | 200                            |
| 30-6, 5-7                        | 450        | 0.03                          | 200                            |
| 32-4, 41-43                      | 500        | 0.1                           | 70                             |
| 52-3, 24-26                      | 800        | 0.4                           | 250                            |
| 60-1, 44-46                      | 400        | 0.1                           | 100                            |
| 67-1, 142-144                    | 500        | 0.05                          | 900                            |
| 67-3, 7-9                        | 500        | 0.1                           | 500                            |
| 71-1, 143-145                    | 700        | 0.05                          | 500                            |
| 72-3, 131-133                    | 900        | 0.1                           | 400                            |
| 74-3, 89-91                      | 700        | 0.2                           | 1150                           |
| 77-1, 69-71                      | 700        | 0.5                           | 2100                           |
| 81-2, 14-16                      | 300        | 0.1                           | 20                             |
| 84-3, 40-42                      | 450        | 0.01                          | 35                             |
| 87-1, 61-63                      | 600        | 0.05                          | 50                             |
| 88-1, 131-137                    | 1800       | 0.8                           | 400                            |
| 90-4, 40-42                      | 2100       | 0.7                           | 250                            |
| 91-3, 45-47                      | 2200       | 0.9                           | 500                            |
| 92-3, 33-35                      | 2150       | 0.9                           | 400                            |
| 93-1, 35-37                      | 2100       | 0.4                           | 300                            |
| 94-1, 57-59                      | 2100       | 0.9                           | 400                            |
| 95-1, 69-71                      | 2200       | 0.35                          | 1100                           |
| 98-5, 74-76                      | 500        | 0.02                          | 50                             |
| 104-1, 13-15                     | 500        | 0.02                          | 130                            |
| 104-1, 50-52                     | 3100       | 0.4                           | 60                             |
| 104-1, 78-80                     | 3000       | 0.9                           | 500                            |
| 104-1, 91-93                     | 3100       | 0.4                           | 500                            |
| 104-1, 112-114                   | 3100       | 0.25                          | 350                            |
| 105-3, 22-24                     | 2800       | 1.15                          | 1700                           |
| 106-1, 63-65                     | 2600       | 0.9                           | 1400                           |
| 108-1, 144-146                   | 2700       | 1.56                          | 1000                           |
| 110-4, 83-85                     | 700        | 0.25                          | 140                            |
| 112-2, 76-78                     | 400        | 0.1                           | 40                             |
| 113-2, 32-34                     | 200        | 0.1                           | 200                            |
| 114-2, 71-73                     | 3300       | 0.25                          | 150                            |
| 118-1, 34-36                     | 3600       | 0.4                           | 700                            |
| 125-1, 120-122                   | 300        | 0.2                           | 20                             |
| 127-4, 138-140                   | 100        | 115                           | 177,000*                       |

Note: HC = coercive field; Jr = natural remanent magnetization intensity; Jrs = saturation remanent intensity.  
\* = rust flake from drill pipe scale.

3D). CS of all samples studied have sharp maxima in the field between 200 and 500 Oe, typical for multidomain magnetites with grains of different sizes.

Sample 515B-46-1, 41-43 cm (Group 1) has a maximum coercive spectrum (CS) in the field of about 400 Oe (Hcr of this sample before heating was 545 Oe); the right branch of CS curve is less sharp than the left one and is skewed to fields of 1200-1500 Oe, indicating weak oxidation. Sample 515B-46-5, 89-91 cm (Group 2), besides having a sharp maximum in the field of 200 Oe, also has a weakly expressed maximum in the field of about 1600 Oe (Fig. 2D). The second maximum may belong to hematite, traces of which are recorded on thermomagnetic curves. In this case, hematite may have an origin independent of magnetite. An almost symmetric CS curve and the presence of a separate maximum near 1600 Oe argues in favor of this supposition. Formation and destruction of new ferromagnetic grains probably occurs in nature, and some of the resulting grains are probably hematite, but we cannot exclude the possibility that the hematite or a part of it may be primary.

Sample 515B-38-4, 87-89 cm was almost unchanged by laboratory heating (Fig. 2). The thermomagnetic analysis (TMA) curves show the presence of hematite. The wide maximum and skewed slope of the right branch of the CS curve points to magnetite grains of different sizes and intensive development of processes that oxidize magnetite to hematite.

The Tc of Sample 516F-33-3, 92-94 cm is offset to 600°C; its Hcr = 600 Oe. The paramagnetic form of the TMA curves of Samples 516F-63-4, 102-104 cm; 516F-65-1, 15-17 cm; and 516F-86-2, 92-94 cm (Hcr = 880, 950, and 1200 Oe, respectively) hardly reveals a Tc near to that of magnetite (580°C). The TMA curve of Sample 516F-109-1, 80-82 cm is paramagnetic, and its saturation parameters show the presence of hydroxides.

These samples have sharp maxima of their CS curves in the region characteristic of magnetite and right branches skewed to 1.5 kOe (Sample 516F-33-3, 92-94 cm), to 3 kOe (Sample 516F-65-1, 15-17 cm), and to 4 kOe (Sample 516F-86-2, 92-94 cm), probably a result of increasing of oxidation processes with increasing depth.

The CS of Sample 516F-63-4, 102-104 cm, the ferromagnetic fraction of which was unchanged by laboratory heating, is more complicated. The absence of distinct signs of hematite does not allow us to relate the maximum near 800 Oe to hematite. Perhaps it is very fine-grained magnetite or second-generation magnetite? Oxidation of magnetite to hematite is reflected in the skewed right branch of CS curve, which reaches 3 kOe.

As the CS of Sample 516F-109-1, 80-82 cm shows, for sediments with paramagnetic TMA curves, each also has a distinct maximum in its CS. That maximum could belong to magnetite. The presence of hydroxides is reflected in right branch of CS, which stretches to more than 7 kOe.

The analysis of CS curves shows a subordinate position of hematite compared to magnetite and the obvious presence of magnetite in the deeper sediments of this

region. Thus, analysis of the CS curves confirms that the chief ferromagnetic mineral in the studied rocks is magnetite, with some hematite present in a number of samples.

In order to identify which mineral is the NRM carrier, the NRM intensity was measured at the Morin transition and at the isotropic point of magnetite. For this purpose, the samples were first cooled to melting temperature for solid CO<sub>2</sub> (-80°C) and then to the temperature of liquid nitrogen (-196°C). J<sub>rs</sub> was measured by the same procedure, for control.

The good agreement between the results of thermomagnetic analysis and that of J<sub>rs</sub> cooling (Table 2) allows us to accept with confidence the results of the samples' cooling. NRM of Samples 515B-40-4, 93-95 cm; 516F-101-1, 119-121 cm; 515B-44-3, 93-95 cm; and 516F-31-5, 20-22 cm can be attributed to magnetite (Table 2). As for Sample 515B-48-4, 134-136 cm, hematite probably plays a significant role in NRM, but no role was discovered for it in the J<sub>rs</sub> curves. In other words, the main ferromagnetic mineral, magnetite, is also the main NRM carrier, although in a number of cases hematite can be a carrier of a rather significant part of NRM.

As shown above, the minerals, particularly magnetite, in our samples are probably primary and of detrital or chemical origin.

The detrital nature of the NRM (and consequently of magnetite) can be supposed according to the following considerations. (1) J<sub>ri</sub> (anhysteretic remanent magnetization) was created in a field nearly equal to the Earth's (0.3 Oe) but has 10 times as much value as J<sub>r</sub> (= NRM) of corresponding samples. (2) For multidomain grains (magnetite in studied samples most probably is multidomain), the CRM increases with increasing H<sub>cr</sub> (with decreasing grain size). CRM properties are still poorly known, but general points of view of CRM origin and a number of experiments argue in favor of such a regularity (Vigilanskaya and Tretjak, 1974). For a wide range

of grain sizes, DRM is not dependent on size. The lack of dependency of I<sub>r</sub>/I<sub>rs</sub> on H<sub>cr</sub> is also evident (Fig. 7) and that, in the authors' opinion, favors an detrital origin of NRM for most of the sediments studied.

The main ferromagnetic mineral in the rocks under consideration is magnetite. It is mainly fine grained but multidomain. Hematite is likely to result from magnetite oxidation, or disintegration of paramagnetic minerals, or may be of primary origin. Generally, the oxidation processes are of variable intensity throughout the sediment column, but in Hole 516F oxidation increases with age. Abundant hydroxides characterize the Cretaceous sediments of Hole 516F. Conditions in some layers lead to the formation of unstable ferromagnetic minerals which in turn disintegrate to hematite. Magnetite is the main carrier of NRM, which most probably is DRM, therefore NRM can be used for magnetostratigraphic investigations.

DISCUSSION

Analyses of J<sub>rs</sub> and H<sub>cr</sub>, indicators of the change of composition and quantities of ferromagnetic minerals with sub-bottom depth in Hole 516F located on the Rio Grande Rise (Fig. 8), leads to the following conclusions:

1) The concentration of the ferromagnetic fraction in Lithologic Units 7 and 8 is different, but the composition of that fraction is obviously similar; in both units, magnetite is the main component.

2) Relatively high values of H<sub>cr</sub> characterize Lithologic Subunits 5b, 6a, and 6b. At the same time, magnetic characteristics allow us to make more detailed subdivisions of these units into horizons (Fig. 8). In a number of cases, the boundaries of the horizons based on magnetic data do not coincide with those based on lithology (Barker et al., 1981).

Most of Lithologic Subunit 6b can be identified by the low values of J<sub>rs</sub> and high values of H<sub>cr</sub> (Fig. 8a). Meanwhile, the upper part of Subunit 6b and lower part of Subunit 6a form one horizon with decreased values of both J<sub>rs</sub> and H<sub>cr</sub>. Subunit 6A can be divided into three horizons: one with increased values of J<sub>rs</sub> and H<sub>cr</sub>, one with decreased values of J<sub>rs</sub> and H<sub>cr</sub>, and one

Table 2. Magnetization (J<sub>rs</sub> and J<sub>r</sub>) changes after cooling in order to control the presence of magnetic and hematite.

| Hole | Core-section (interval in cm) | J <sub>r</sub> × 10 <sup>-5</sup> emu <sup>a</sup> |      |      | J <sub>rs</sub> × 10 <sup>-5</sup> emu <sup>b</sup> |       |       |
|------|-------------------------------|--|------|------|---|-------|-------|
|      |                               | T  | C1   | C2   | T   | C1    | C2    |
| 515B | 36-1, 48-50                   |  |      |      | 108.5   | 107.5 | 100.0 |
|      | 40-2, 41-42                   |  |      |      | 119.0   | 116.5 | 111.0 |
|      | 40-4, 93-95                   | 2.62   | 2.60 | 2.18 |   |       |       |
|      | 44-3, 93-95                   | 1.90   | 1.78 | 1.61 |   |       |       |
|      | 45-2, 49-51                   |  |      |      | 64.5  | 64.5  | 60.0  |
|      | 48-4, 134-136                 | 1.11   | 1.00 | 0.93 |   |       |       |
|      | 49-1, 140-142                 |  |      |      | 56.0  | 56.0  | 52.0  |
| 516F | 55-1, 3-5                     |  |      |      | 64.0  | 63.5  | 59.5  |
|      | 19-2, 103-105                 |  |      |      | 25.0  | 24.5  | 23.5  |
|      | 31-5, 20-22                   | 0.43   | 0.39 | 0.27 |   |       |       |
|      | 32-4, 41-43                   |  |      |      | 17.0  | 16.5  | 15.5  |
|      | 52-3, 24-26                   |  |      |      | 71.0  | 66.5  | 64.5  |
|      | 87-1, 61-63                   |  |      |      | 11.0  | 10.5  | 10.0  |
|      | 101-1, 119-121                | 0.28   | 0.27 | 0.18 |   |       |       |
|      | 104-1, 78-80                  |  |      |      | 74.0  | 70.5  | 68.0  |
|      | 127-4, 138-140                |  |      |      | 133.0   | 125.5 | 112.5 |

Note: T = temperature is 20°C; C1 = after cooling to -80°C; C2 = after cooling to -196°C; a blank indicates that no value was available.

<sup>a</sup> After heating to 230°C.

<sup>b</sup> H = 10<sup>3</sup> Oe.

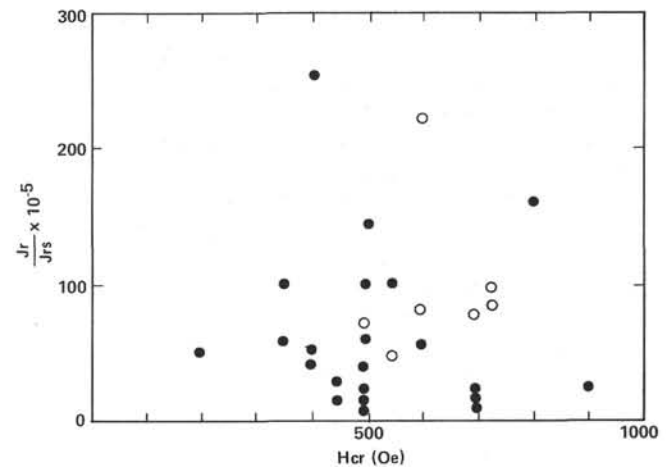


Figure 7. Remanent coercive force (H<sub>cr</sub>) versus the value of remanent magnetization (J<sub>r</sub>) normalized to saturation remanent magnetization (J<sub>rs</sub>).

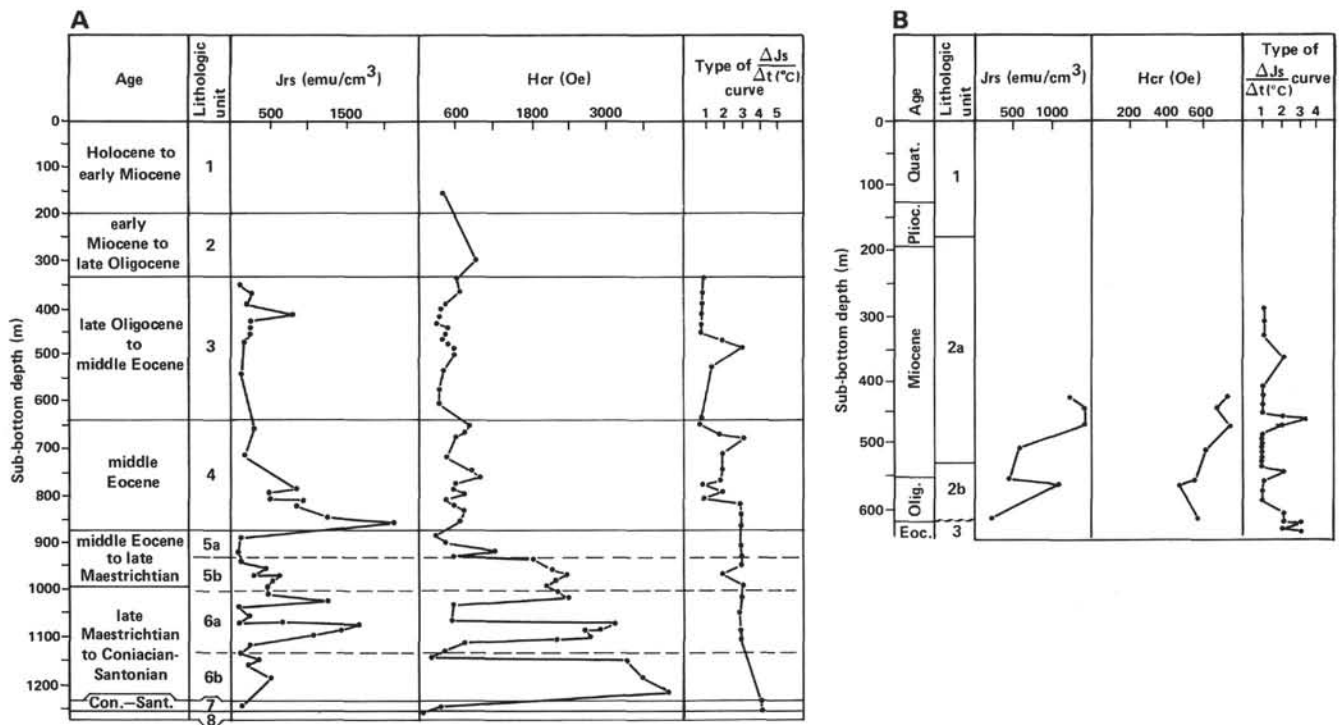


Figure 8. Variation of magnetic characteristics of samples from Holes 515B (8A) and 516F (8B). Jrs = saturation remanent magnetization, Hcr = remanent coercive force,  $\Delta J_s$  = rate of change of saturation magnetization, t = temperature.

with increased Hcr and average values of Jrs. The last horizon, beginning in upper part of this unit, continues up to the upper boundary of Subunit 5b. Very low values of Jrs and low values of Hcr characterize Subunit 5a and distinguish it from the sediments of neighboring lithologic units.

3) Several new horizons, whose differences are not as obvious as previous ones, are distinguished in the remaining lithologic units. The rocks of the lower half of Unit 4 are exceptions in their higher Jrs values. All sediments of Unit 4 (middle Eocene) have somewhat higher values of Hcr compared with those of Unit 3 (middle Eocene to upper Oligocene).

Sharp changes of Jrs and Hcr occur in all Hole 516F lithologic units, between Unit 8 and up to the middle of Unit 4. The presence of hydroxides is characteristic for all these rocks, but oxidizing conditions are different for this part of section in comparison with the upper part of the hole. Unit 3 and the upper part of Unit 4 have the same ferromagnetic fraction composition. Types 1 and 2 of  $\Delta J_s/\Delta t$  curves differ from each other only by the intensity of change of laboratory heating. Concentration of the ferromagnetic fraction in Units 3 and 4 of Hole 516F varies only slightly; changes of Hcr are of regular character (Hcr changes twice), and they are evidence of a change in the size of the magnetite grains. The regularity of these alternations allows us to suppose that they were associated with changing exterior conditions.

**ACKNOWLEDGMENTS**

The authors are very grateful to N. Hamilton and A. Suzyumov for sharing their samples, to B. Burov and P. Yasonov for assistance in carrying out the experiments, to G. Pospelova and V. Vadkovsky for their peer reviews of the article, as well as to W. Coulbourn for his assistance.

**REFERENCES**

Bagin, V. I., Gendler, T. S., Rybak, R. S., and Kizmin, R. N., 1974. Temperature transitions of natural solid solution (Fe, Mg)CO<sub>3</sub>. *Izv. Akad. Nauk Arm. SSR, Fiz. Zemli*, 6:73-84. (in Russian)

Barker, P. F., Carlson, R. L., Johnson, D. A., and Shipboard Scientific Party, 1981. Deep Sea Drilling Project Leg 72: southwest Atlantic paleocirculation and Rio Grande Rise tectonics. *Bull. Geol. Soc. Am.*, Pt. 1, 92:294-309.

Burov, B. V., and Yasonov, P. G., 1979. Introduction in differential thermomagnetic analysis of rocks. Kazan State University, Kazan City. (in Russian)

Petrova, G. N., 1977. Laboratory methods at paleomagnetic investigations. *Geomagnetic Collection of Papers*, 19:40-49.

Rybak, R. S., 1971. About diagnostics of maghemite by thermomagnetic method. *Izv. Akad. Nauk. Arm. SSR, Fiz. Zemli*, 4:98-101. (in Russian)

Vigilianskaya, L. I., and Tretiak, A. N., 1974. Some parameters of chemical remanent magnetization and their changes in heating process. *Geophysics Collection of Papers of AN Ukrainian SSR*, 57:76-82. (in Russian)

Date of Initial Receipt: September 7, 1982